

RAILROAD NOISE AFFECTED BY DOWNWARD REFRACTION AND TURBULENCE

R. GOŁĘBIEWSKI^(*) and R. MAKAREWICZ

Institute of Acoustics
A. Mickiewicz University
61-614 Poznań, Umultowska 85
Poland

For downward ray bending (temperature inversion and/or downwind propagation) geometrical spreading is principally affected by atmospheric turbulence. Additionally, the variations of rolling stock and train speed occur. Thus, the sound exposure level, L_{AE} , changes from train to train and the equivalent continuous A-weighted sound pressure level of railroad noise, L_{AeqT} , changes from day to day. As such, the mean, \bar{L}_{AeqT} , is important environmental noise characteristics. The simplified model of noise generation and propagation is derived. It makes possible to calculate \bar{L}_{AeqT} . Two adjustable parameters of the model are estimated from measurements of the sound exposure level, L_{AE} .

1. Introduction

For upward ray bending (temperature lapse and/or upwind propagation) geometrical spreading of train noise is affected strongly by refraction [1, 2]. When temperature increases with height (e.g., at evening and night after a sunny day), ray paths curve downward. Similar phenomenon occurs during downwind propagation. In such a case, the interaction with the ground surface, i.e., ground effect, can be neglected. This conclusion can be proved theoretically [3–8] and experimentally [9, 10] for any type of ground surface, either soft or hard. Under such circumstances, the only result of the ground effect on train noise is the virtual change of the A-weighted sound power, W_A , that comes from the reflection by the stone bedding, $W_A \rightarrow \beta \cdot W_A$ (for a hard surface we obtain $\beta \approx 2$).

In the present study we assume that during downward propagation geometrical spreading is modified mainly by refraction and atmospheric turbulence. Thus, the process of noise propagation has a stochastic nature.

Due to differences among the cars and different speeds of trains belonging to the same category (inter-city, passenger, freight, etc.), the process of noise generation is stochastic as well. Therefore, the time patterns of noise from a single train, and the corresponding values of the relative sound exposure, e (Sec. 2), are random (Fig. 1).

^(*) Corresponding author (e-mail: roman_g@amu.edu.pl)

Finally, the equivalent continuous A-weighted sound pressure level for each day are not the same: $L_{AeqT}^{(i)}$, $i = 1, 2, \dots, 30, \dots, 365, \dots$. This study derives the mean \bar{L}_{AeqT} , as function of the perpendicular distance from the track, D .

Many theoretical models of sound propagation in a turbulent medium have been proposed (see [11] and the literature cited therein). Although it would be possible to calculate \bar{L}_{AeqT} using these models, the associated computations would be cumbersome and tedious. Additionally, to make these results applicable in practice, not only noise measurements but meteorological measurements at each site of interest are needed. Unfortunately, the meteorological equipment (temperature sensors, anemometers, signal conditioning modules, data recording computers, etc.) is not available everywhere. Therefore, need for a less sophisticated and simpler theory has arisen.

This study proposes a method of predicting $\bar{L}_{AeqT}(D)$ which requires only noise measurements at two locations.

An heuristic theory of noise generation and propagation is presented in Sec. 2. Section 3 verifies the theory with measurements of the sound exposure level, L_{AE} . Finally, Sec. 4 calculates the average value of the equivalent continuous A-weighted sound pressure level.

2. Noise generation and propagation

A single noise event, i.e., a train passing by, can be quantified by the relative sound exposure,

$$e = \frac{E}{p_o^2 t_o}, \quad p_o = 20 \text{ } \mu\text{Pa}, \quad t_o = 1 \text{ s}, \quad (1)$$

where the sound exposure, E , is the integral over the A-weighted squared sound pressure,

$$E = \int_{-\infty}^{\infty} p_A^2(t) dt. \quad (2)$$

For N trains belonging to the same category (inter-city, passenger, freight, etc.) passing the receiver during the sample time, T , the equivalent continuous A-weighted sound pressure level is written in the following form:

$$L_{AeqT} = 10 \lg \left\{ \frac{N t_o}{T} e \right\}. \quad (3)$$

In reality, due to stochastic nature of noise generation and propagation, the relative sound exposure, e (Fig. 1), may be different for each train. Thus, the average value of the of the equivalent continuous A-weighted sound pressure level is,

$$\bar{L}_{AeqT} = 10 \lg \left\{ \frac{N t_o}{T} \bar{e} \right\}, \quad (4)$$

where

$$\bar{e} = \lim_{N \rightarrow \infty} \left\{ \frac{1}{N} \sum_{j=1}^N e_j \right\}. \quad (5)$$

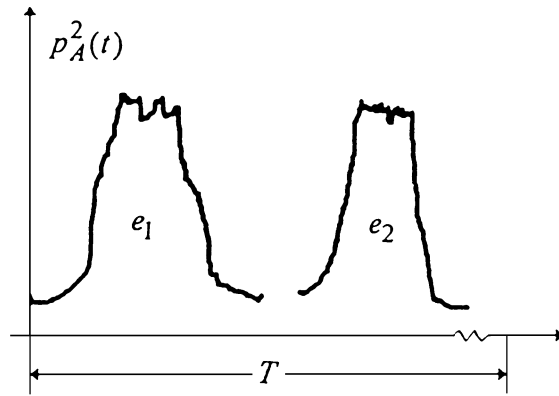


Fig. 1. Time variations of the A-weighted squared sound pressure, p_A^2 , and the noise events described in terms of the relative sound exposure, e (Eq. (1)).

Now we calculate the relative sound exposure, e (Eqs. (1), (2)). A moving train can be modeled by a line source consisting of directional point sources [12-16]. Due to the uniformity of line source, the linear density of the A-weighted sound power, W_A (expressed in *Watts per meter*), can be employed. Because of turbulence, the only result of the ground effect is the virtual change of the sound power, $W_A \rightarrow \beta \cdot W_A$ (see Introduction). As the noise propagates in a real atmosphere, due to refraction and turbulent eddies, the rays are no longer straight lines. Consequently, the ray tube is no longer a cone with the cross-section (Fig. 2)

$$\Delta S_o = r^2 \Delta \Omega, \quad (6)$$

where $\Delta \Omega$ is a solid angle and r is the distance between the source, S , and receiver, O . The eddies and refraction modify the cross-section area, $\Delta S_o \rightarrow \Delta S$, where

$$\Delta S = r^2 \Delta \Omega \cdot [1 + \sigma(t) \cdot r]^2. \quad (7)$$

The random function $\sigma(t)$ integrates the influence of all encountered eddies and refraction over the path of propagation, r . For $\sigma < 0$ and $\sigma > 0$ we get the phenomena of focusing

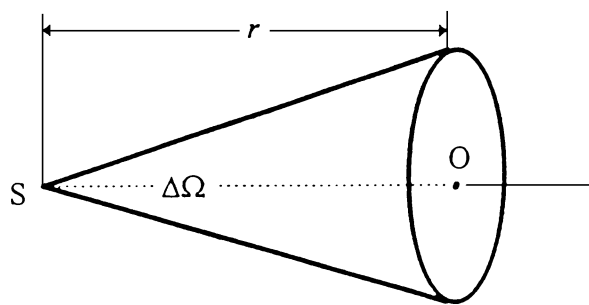


Fig. 2. Ray tube made of straight rays in an ideal atmosphere (calm and homogeneous).

and defocusing of rays, respectively, thus σ is the propagation parameter responsible for noise fluctuation. Using the exact theory [11], one can determine the relationship between σ and the temperature and wind profiles, or between the fluctuating index of refraction and the parameters describing the turbulence structure. For engineering purposes, however, such a relationship is not useful because these characteristics are rarely available at the site of interest, where the prediction of $\bar{L}_{AeqT}(D)$ must occur. In Sec. 3 we will introduce the adjustable parameter χ , which is related to $\sigma(t)$. Now we make use of the energy conservation law [17],

$$I_A^{(o)} \cdot \Delta S_o = I_A \cdot \Delta S, \quad (8)$$

where $I_A^{(o)}$ and I_A denote the A-weighted sound intensity in an ideal (homogeneous and motionless) and real (refractive and turbulent) atmosphere, respectively. In an ideal atmosphere, far away from the unit length line source, $r \gg l_o = 1$ m, one can be write [12-16],

$$I_A^{(o)} = \frac{W_A l_o}{r^2} Q(\Theta), \quad (9)$$

where W_A is the linear density of the A-weighted sound power, $Q(\Theta)$ describes the source directivity, and Θ expresses the angle between the source-receiver line, SO , and the y axis (Fig. 3). For near-grazing propagation, the source-receiver distance, r , and the angle, Θ , can be replaced by the horizontal distance, d , and the angle, Φ , respectively (Fig. 4). Combining Eqs. (7)–(9) yields the A-weighted squared sound pressure in a turbulent atmosphere,

$$p_A^2 = \frac{\beta W_A l_o \rho c}{d^2 [1 + \sigma \cdot d]^2} F(\Phi), \quad (10)$$

where σ accounts for refraction and turbulence scattering. Here β describes reflection from the stone bedding and ρc is the characteristic impedance of air.

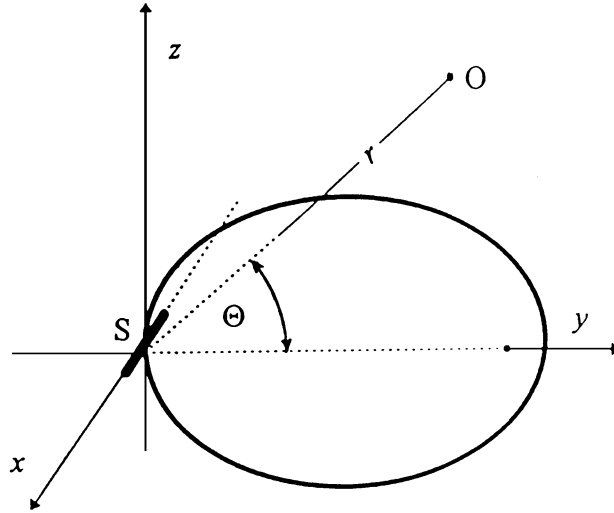


Fig. 3. Radiation pattern of a line source of unit length (Eq. (9)).

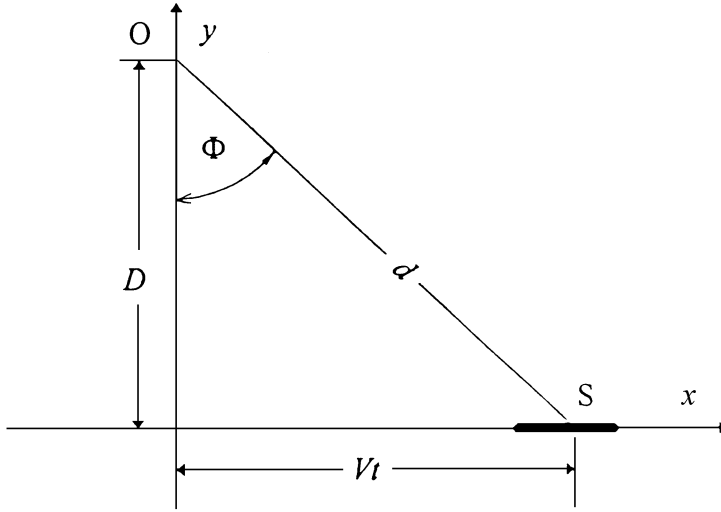


Fig. 4. Perpendicular distance, D , and the angle, Φ , determining the instantaneous location of a moving source.

To verify this equation, first the sound exposure level, L_{AE} , for a line source made of point sources (Eq. (10)) is calculated. Then, the results of calculations are compared with field measurements.

3. Sound exposure level

The definition of the sound exposure level is

$$L_{AE} = 10 \lg\{e\}, \quad (11)$$

where the relative sound exposure, e , is proportional to the sound exposure, E (Eq. (1)). If the uniform line source of length, l , moves with a steady speed, V , along the x axis from $x = -\infty$ to $x = +\infty$, at the perpendicular distance, D , from the receiver (Fig. 4), then [12-16]

$$E = \frac{Dl}{Vl_o} \int_{-\pi/2}^{+\pi/2} \frac{p_A^2(\Phi)}{\cos^2 \Phi} d\Phi. \quad (12)$$

Note that the limits of integration corresponds to downward refraction (the hole track participates in noise reaching the receiver). Before we proceed with further calculations, we introduce the linear density of sound energy, $W_A l/V$ [1]. Accordingly, the reference value of the linear density of sound energy is $P_o l_o/V_o$, where $P_o = 10^{-12}W$ and $V_o = l_o/t_o$. Consequently, the quantity

$$\mu = \beta \frac{W_A l}{V} / \frac{P_o l_o}{V_o}, \quad (13)$$

can be interpreted as the relative density of sound energy that is modified by the reflection from a stone bedding (β). In this way three parameters describing the noise source (W_s , V , and l), are replaced by only one, μ .

To determine the parameter σ (Eq. (10)) that describes noise propagation, Eq. (12) must first be integrated. Inserting the A-weighted squared sound pressure (Eq. (10)) we arrive at the relative sound exposure (Eq. (1)),

$$e = \mu \frac{l_o}{D} \cdot J_\sigma(D), \quad (14)$$

where the influence of refraction and turbulence is given by the integral,

$$J_\sigma(D) = \int_{-\pi/2}^{+\pi/2} F(\Phi) \cdot \left[1 + \frac{\sigma(\Phi)}{\cos \Phi} D \right]^{-2} d\Phi. \quad (15)$$

Note that for a nonrefractive and nonturbulent atmosphere, with $\sigma = 0$, we get

$$J_o = \int_{-\pi/2}^{+\pi/2} F(\Phi) d\Phi, \quad (16)$$

and the relative sound exposure, e (Eq. (14)), is inversely proportional to the perpendicular distance, D . Consequently, there is a drop of the sound exposure level per doubling of the distance, $L_{AE}(D) - L_{AE}(2D) = 3$ dB (Eqs. (11), (14), (16)).

The ray tube carries noise from the source, S , to the receiver, O . In the real atmosphere, during the train motion from $x = -\infty$ ($\Phi = -\pi/2$) to $x = +\infty$ ($\Phi = +\pi/2$), the ray tube encounters different eddies that change its cross-section. This is the rationale used to write σ as a function of the angle Φ (Eq. (15)). To calculate $J_\sigma(D)$, we apply the mean value theorem of integral calculus [18],

$$J_\sigma(D) = \left[1 + \frac{\sigma(\tilde{\Phi})}{\cos \tilde{\Phi}} D \right]^{-2} \cdot J_o, \quad (17)$$

where $0 < \tilde{\Phi} < 2\pi$ and J_o is defined by Eq. (16). With the *propagation parameter*, $\chi = \sigma(\tilde{\Phi})/\cos \tilde{\Phi}$, the sound exposure level is (Eqs. (11), (14), (17))

$$L_{AE} = 10 \lg \left\{ \eta \frac{l_o}{D} [1 + \chi \cdot D]^{-2} \right\}, \quad (18)$$

where the *generation parameter* is, $\eta = J_o \mu$. In the real atmosphere, the values of η and χ are modified slightly by ground effect and air absorption.

To determine χ and η , one needs two simultaneous measurements of the sound exposure level, $L_{AE}(D_1)$ and $L_{AE}(D_2)$. Considering the above equation as a theoretical prediction with adjustable parameters, we obtain

$$\chi = \frac{k - 1}{D_2 - kD_1}, \quad (19)$$

where

$$k = \sqrt{\frac{D_1}{D_2}} 10^{[L_{AE}(D_1) - L_{AE}(D_2)]/20}, \quad (20)$$

is available from the measurements taken. By substituting χ into Eq. (18), we arrive at the generation parameter, η .

If during the sources, motion the process of focusing prevails, then $\chi < 0$ and the decrease of the sound exposure level with doubling of the distance is less than 3 dB. In the opposite case, when defocusing predominates, the decrease exceeds 3 dB. This is exactly what we obtained from noise measurements (Figs. 5, 6).

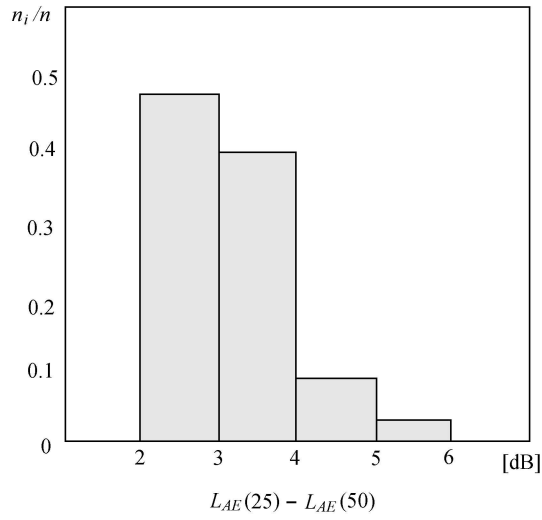


Fig. 5. Probability distribution of the sound level decrease per doubling of the distance, $L_{AE}(25) - L_{AE}(50)$, with the total number of measurements, $n = 37$.

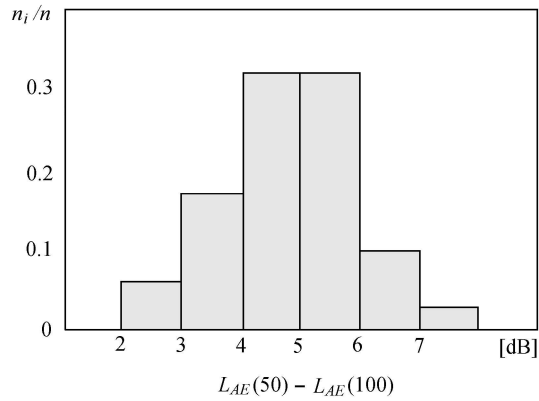


Fig. 6. Probability distribution of the sound level decrease per doubling of the distance, $L_{AE}(50) - L_{AE}(100)$, with the total number of measurements, $n = 37$.

Example

Noise was generated by a commuter train, Fukuoka-Omuta (Japan), moving with steady speed on a 1 m high embankment. The site was a wide-open agriculture area. Varying wind was blowing along the track with the average velocity less than 2 [m/s]. Thirty-seven measurements of the sound exposure level, $L_{AE}(D)$, were simultaneously taken at three distances, $D = 25, 50,$ and 100 m, with microphones at a height of 1 m (Table I). The sound level decrease per doubling of the distance, $L_{AE}(25) - L_{AE}(50)$, is shown in Fig. 5, and for $L_{AE}(50) - L_{AE}(100)$ in Fig. 6. In both figures the decrease is greater and sometimes less than 3 dB, corresponding to the negative and positive values of the parameter of propagation, χ (Eq. (18)), respectively.

To determine χ and η , we used $L_{AE}(25)$ and $L_{AE}(100)$, i.e., the results of measurements at distances $D_1 = 25$ m and $D_2 = 100$ m. Calculation results (Eqs. (19), (20)) are shown in Table 1.

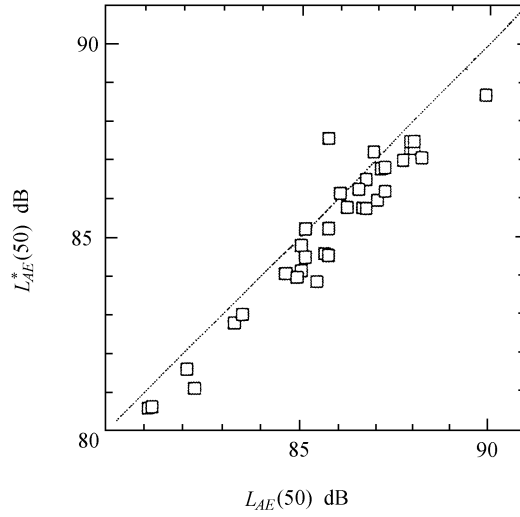


Fig. 7. Calculated and measured values of the sound exposure level, $L_{AE}^*(50)$ and $L_{AE}(50)$, with the average difference, -0.6 dB.

To verify the simplified theory of noise generation and propagation (Eq. (10)), we used Eq. (18) to predict the sound exposure level at the distance, $D = 50$ m. Both values, measured and predicted sound exposure levels, $L_{AE}(50)$ and $L_{AE}^*(50)$, are listed in Table I and plotted in Fig. 7. The diagonal line indicates the ideal relationship between the two levels in which the prediction corresponds exactly to the measurement. The difference, $L_{AE}^*(50) - L_{AE}(50)$, ranges from an under-prediction of -1.6 dB to an over-prediction of $+1.8$ dB. The mean error for 37 measurements is relatively small, -0.6 dB. Thus, within 100 m of the track, the theory is in satisfactory agreement with experimental values.

Table 1. Simultaneously measured sound exposure levels, $L_{AE}(25)$, $L_{AE}(50)$, $L_{AE}(100)$, and the calculated sound exposure level, $L_{AE}^*(50)$ (Eq. (18)). Parameters η and χ are calculated from equations (18)–(20)

$L_{AE}(25)$	$L_{AE}(50)$	$L_{AE}(100)$	$\chi [10^{-4}]$	$\eta [10^9]$	$L_{AE}^*(50)$
89.5	86.0	82.4	18.46	24.40	86.1
89.6	87.1	84.0	-6.20	22.11	86.7
88.1	85.1	82.4	-4.77	15.77	85.2
90.3	87.9	84.2	1.23	26.97	87.3
83.1	80.7	76.2	14.73	5.49	79.8
89.5	86.7	83.4	1.23	22.43	86.5
91.1	85.7	83.5	28.48	36.98	87.5
89.1	86.6	82.0	18.46	22.25	85.7
85.4	82.1	77.2	42.02	10.59	81.6
88.6	85.6	79.8	57.51	23.70	84.6
91.4	87.9	82.8	52.11	44.11	87.4
87.4	85.0	80.6	12.92	14.65	84.1
90.1	87.7	83.7	6.04	26.37	87.0
89.9	86.5	82.0	35.03	28.91	86.2
86.7	83.3	78.2	49.50	14.78	82.8
89.6	87.0	81.7	35.03	26.98	85.9
90.6	86.9	83.4	20.38	31.72	87.2
88.0	85.7	80.6	24.35	17.76	84.5
90.5	88.0	83.8	11.15	29.65	87.3
89.5	86.2	81.4	39.64	26.93	85.7
84.1	81.1	76.7	24.35	7.23	80.6
89.5	86.7	81.3	42.02	27.22	85.7
88.2	85.4	78.6	81.92	23.99	83.8
90.2	88.2	83.7	7.71	27.21	87.0
92.3	89.9	84.5	32.80	49.73	88.7
87.4	84.6	80.4	16.57	14.91	84.1
84.9	82.3	76.7	42.02	9.44	81.1
88.3	85.1	80.0	44.46	20.88	84.5
84.0	80.6	72.6	160.14	12.32	78.8
90.9	88.0	83.6	22.34	34.31	87.4
89.6	85.0	79.0	120.43	38.62	84.8
85.0	81.2	75.4	81.92	11.48	80.6
90.4	87.2	81.1	72.20	38.22	86.2
88.5	84.9	78.5	96.10	27.24	84.0
89.9	87.2	83.5	6.04	25.19	86.8
89.7	85.7	79.8	92.42	35.37	85.2
87.5	83.5	77.6	92.42	21.32	83.0

4. Equivalent continuous a-weighted sound pressure level

Noise events associated with passing trains are quantified by the relative sound exposures, e (Eq. (1)). For the j -th train, we can write (Eqs. (11), (18))

$$e(\mu_j, \chi_j) = \eta_j \frac{l_o}{D} [1 + \chi_j D]^{-2}. \quad (21)$$

The values of η_j and χ_j are random (see Table I), so we write

$$\eta_j = \bar{\eta} + \delta\eta_j, \quad \chi_j = \bar{\chi} + \delta\chi_j, \quad (22)$$

where $\bar{\mu}$ and $\bar{\chi}$ denote the population means that represents an infinite number of trains. If the variations of the propagation parameter meet the condition

$$\left| \frac{\delta\chi_j \cdot D}{1 + \bar{\chi} \cdot D} \right| < 1, \quad (23)$$

then

$$e(\eta_j, \chi_j) \approx e(\bar{\eta}, \bar{\chi}) \cdot \left[1 + \frac{\delta\eta_j}{\bar{\eta}} - 2R \left(\frac{\delta\chi_j}{\bar{\chi}} + \frac{\delta\chi_j}{\bar{\chi}} \frac{\delta\eta_j}{\bar{\eta}} \right) + 3R^2 \left(\frac{\delta\chi_j}{\bar{\chi}} \right)^2 \right], \quad (24)$$

where $e(\bar{\eta}, \bar{\chi})$ is the relative sound exposure calculated for the mean values $\bar{\mu}$ and $\bar{\chi}$ (Eq. (21)), and

$$R = \frac{\bar{\chi} \cdot D}{1 + \bar{\chi} \cdot D}. \quad (25)$$

Making use of Eq. (24), we get the population mean of the relative sound exposure,

$$\bar{e} \approx (\bar{\eta}, \bar{\chi}) \cdot [1 - 2m_{\eta\chi}R + 3m_{\chi\chi}R^2], \quad (26)$$

where the estimates of the moments $m_{\eta\chi}$ and $m_{\chi\chi}$ are

$$m_{\eta\chi} = \frac{1}{n} \sum_{j=1}^n \left(1 - \frac{\eta_j}{\bar{\eta}} \right) \left(1 - \frac{\chi_j}{\bar{\chi}} \right), \quad (27)$$

and

$$m_{\chi\chi} = \sum_{j=1}^n \left(1 - \frac{\chi_j}{\bar{\chi}} \right)^2. \quad (28)$$

For example, taking 37 values of η_j and χ_j from Table I, we obtain

$$\bar{\eta} = 2.43 \cdot 10^{10}, \quad \bar{\chi} = 4.04 \cdot 10^{-3}, \quad m_{\eta\chi} = 0.0291, \quad \text{and} \quad m_{\chi\chi} = 0.834.$$

The mean value of the equivalent continuous A-weighted sound pressure level, \bar{L}_{AeqT} , can be calculated from Eq. (4), with the mean sound exposure level given by (Eqs. (11), (26))

$$\bar{L}_{AE}(D) = L_{AE}^{(o)}(D) + \delta L_{AE}(D). \quad (29)$$

Here,

$$L_{AE}^{(O)} = 10 \lg \left\{ \bar{\eta} \frac{l_o}{D} [1 + \bar{\chi}D]^{-2} \right\}, \quad (30)$$

corresponds to geometrical spreading ($\bar{\eta}$) that is modified by rays focusing ($\bar{\chi}$), and

$$\delta L_{AE} \approx 10 \lg \left\{ 1 - 2m_{\eta\chi} \frac{\bar{\chi}D}{1 + \bar{\chi}D} + 3m_{\chi\chi} \left(\frac{\bar{\chi}D}{1 + \bar{\chi}D} \right)^2 \right\}, \quad (31)$$

accounts for the random nature of sound generation and propagation. To obtain the explicit form of $\bar{L}_{AE}(D)$ for the site of interest (Eqs. (29)–(31)), one can use the values of $\bar{\eta} = 2.43 \cdot 10^{10}$, $\bar{\chi} = 4.04 \cdot 10^{-3}$, $m_{\eta\chi} = 0.0291$, and $m_{\chi\chi} = 0.834$. Finally, the mean value of the equivalent continuous A-weighted sound pressure level, \bar{L}_{AeqT} , is given by Eq. (3),

$$\bar{L}_{AeqT} = 10 \lg \left\{ \frac{Nt_o}{T} \right\} \bar{L}_{AE}(D). \quad (32)$$

5. Conclusion

The mean value of the equivalent continuous A-weighted sound pressure level, \bar{L}_{AeqT} (Eq. (32)) is derived as the function of the perpendicular distance from the track, D . This equation can be used when noise propagates downward (temperature inversion and/or downwind propagation) and geometrical spreading is affected by refraction and atmospheric turbulence (e.g. wind eddies). The advantage of the method presented here is its simplicity: it does not require meteorological measurements at the site of interest, only measurements of the sound exposure level, L_{AE} , are necessary.

In many codes of practice, one is not interested in the mean over all weather situations, but within a certain meteorological window. Therefore it seems reasonable to consider four cases: wind blowing along the track with- or without air temperature increase with height, and wind blowing perpendicular to the track with- or without air temperature increase with height.

Acknowledgements

The authors are grateful to K. MASUDA, Y. SATO, M. YOSHIDA, J. KOGA, M. FUJIMOTO, M. IMANISHI, S. MAEDA, and S. TONDA, former students of the Kyushu Institute of Design, for assistance with noise measurements.

References

- [1] R. MAKAREWICZ, *The influence of refraction and turbulence on railroad noise*, J. Sound Vibr., **210**, 367–74 (1998).
- [2] R. MAKAREWICZ, *Impact of refraction on train noise*, Applied Acoustics, **57**, 279–287 (1999).
- [3] W.E. MCBRIDE, H.E. BASS, R. RASPET, and K.E. GILBERT, *Scattering of sound by atmospheric turbulence: A numerical simulation above a complex impedance boundary*, J. Acoust. Soc. Am., **90**, 3314–25 (1991).

-
- [4] R. RASPET and W. WU, *Calculation of average turbulence effect on sound propagation based on the fast field program formulation*, J. Acoust. Soc. Am., **97**, 147–152 (1995).
- [5] A. L'ESPERANCE, Y. GABILLET, and G.A. DAIGLE, *Outdoor sound propagation in the presence of atmospheric turbulence: experiments and theoretical analysis with the fast field program algorithm*, J. Acoust. Soc. Am., **98**, 570–579 (1995).
- [6] P. CHEVRET, PH. BLANC-BENON, and D. JUVE, *A numerical model for sound propagation through a turbulent atmosphere near the ground*, J. Acoust. Soc. Am., **100**, 3587–99 (1996).
- [7] K. ATTENBOROUGH and K.M. LI, *Ground effect for A-weighted noise in the presence of turbulence and refraction*, J. Acoust. Soc. Am., **102**, 1013–22 (1997).
- [8] E.M. SALOMONS, V.E. OSTASHEV, S.F. CLIFFORD, and R.J. LATAITIS, *Sound propagation in a turbulent atmosphere near the ground: An approach based on the spectral representation of the refractive-index fluctuations*, J. Acoust. Soc. Am., **109**, 1881–93 (2001).
- [9] J.E. PIERCY, T.F.W. EMBLETON and L.C. SUTHERLAND, *Review of noise propagation in the atmosphere*, J. Acoust. Soc. Am., **61**, 1403–18, Fig. 16 (1977).
- [10] K. YAMAMOTO and M. YAMASHITA, *Measurements and analysis of sound propagation over lawn*, J. Acoust. Soc. Jap. (E), **15**, 1–12, Fig. 3 (1994).
- [11] V.E. OSTASHEV, *Acoustics in Moving Inhomogeneous Media*, E&FN Spon, London 1997.
- [12] B. HEMSWORTH, *Prediction of train noise*, [in:] *Transportation Noise Reference Book* [Ed.:] P.M. Nelson, Butterworths, London 1987.
- [13] D. HOHENWARTER, *Railway noise propagation models*, J. Sound Vibr., **141**, 17–41 (1990).
- [14] Y. OKUMURA and K. KUNO, *Multiple regression analysis of railway noise based on finite line source model*, J. Acoust. Soc. Jap. (E), **13**, 161–169 (1992).
- [15] R. MAKAREWICZ, K.B. RASMUSSEN, and P. KOKOWSKI, *Ground attenuation of railroad noise*, Acustica/Acta Acustica, **82**, 636–641 (1996).
- [16] R. MAKAREWICZ and M. YOSHIDA, *Railroad noise in open space*, Applied Acoustics **49**, 291–305 (1997).
- [17] A.D. PIERCE, *Acoustics*, McGraw-Hill, New York 1981.
- [18] R. COURANT and F. JOHN, *Introduction to Calculus and Analysis*, Wiley, New York 1965.